Cell And Tissue Research
July 2014, Volume 357 Issue 1 Pages 195-206
http://dx.doi.org/10.1007/s00441-014-1845-5
http://archimer.ifremer.fr/doc/00202/31352/

Differential distribution of V-type H+-ATPase and Na+/K+-ATPase in the branchial chamber of the palaemonid shrimp *Macrobrachium amazonicum*

Boudour-Boucheker Nesrine [1, *], Boulo Viviane [2], Charmantier-Daures Mireille [1], Grousset Evelyse [1], Anger Klaus [3], Charmantier Guy [1], Lorin-Nebel Catherine [1]

[1] Univ Montpellier 2, Equipe Adaptat Ecophysiol & Ontogenese, CNRS IRD Ifremer, UMR5119 EcoSyM,UM2 UM1, F-34095 Montpellier 05, France.
[2] Ifremer, LEAD, Noumea 98846, New Caledonia.
[3] Biol Anstalt Helgoland, Alfred Wegener Inst Polar & Meeresforsch, D-27498 Helgoland, Germany.

* Corresponding author : Nesrine Boudour-Boucheker, email address : nboudour@yahoo.fr

Abstract :

V-H+-ATPase and Na+/K+-ATPase were localized in the gills and branchiostegites of *M. amazonicum* and the effects of salinity on the branchial chamber ultrastructure and on the localization of transporters were investigated. Gills present septal and pillar cells. In freshwater (FW), the apical surface of pillar cells is amplified by extensive evaginations associated with mitochondria. V-H+-ATPase immunofluorescence was localized in the membranes of the apical evaginations and in clustered subapical areas of pillar cells, suggesting labeling of intracellular vesicle membranes. Na+/K+-ATPase labeling was restricted to the septal cells. No difference in immunostaining was recorded for both proteins according to salinity (FW vs. 25 PSU). In the branchiostegite, both V-H+-ATPase and Na+/K+-ATPase immunofluorescence were localized in the same cells of the internal epithelium. Immunogold revealed that V-H+-ATPase was localized in apical evaginations and in electron-dense areas throughout the inner epithelium, while Na+/K+-ATPase occurred densely along the basal infoldings of the cytoplasmic membrane. Our results suggest that morphologically different cell types within the gill lamellae may also be functionally specialized. We propose that, in FW, pillar cells expressing V-H+-ATPase absorb ions (Cl-, Na+) that are transported either directly to the hemolymph space or through a junctional complex to the septal cells, which may be responsible for active Na+ delivery to the hemolymph through Na+/K+-ATPase. This suggests a functional link between septal and pillar cells in osmoregulation. When shrimps are transferred to FW, gill and branchiostegite epithelia undergo ultrastructural changes, most probably resulting from their involvement in osmoregulatory processes.

Keywords : Osmoregulation, Na+/K+-ATPase, V-type H+-ATPase, Gills, Branchiostegite

Introduction

Some crustaceans, in particular palaemonid shrimp, are able to migrate over large distances (Bauer, 2004). These migrations, which are often related to reproduction and development, expose the animals at successive ontogenetic stages to different salinity regimes (Anger, 2001). The species complex collectively referred to as *Macrobrachium amazonicum* is generally considered as an example of highly successful evolutionary invasions into FW environments (Anger 2013, Pileggi et al. 2013). Most populations are found in slowly flowing rivers near the sea, depending on estuarine water for complete larval development (McNamara et al. 1983; Moreira et al. 1986; Anger et al. 2009). Those near-coastal or estuarine populations represent the species *M. amazonicum sensu stricto*, which was originally described by Heller (1862) as *Palaemon amazonicus* from a riverine habitat in the Amazon Delta (type locality in Heller's original description: "Amazon River"; according to labels on syntypes MHMW 562 and 563 deposited at the Naturhistorisches Museum, Vienna: Gurupá, state of Pará, northeastern Brazil; F. Mantelatto, pers. comm.). Other populations currently assigned to the same species are hololimnetic, spending their entire life cycle in land-locked fresh water habitats located up to several thousand kilometers from the sea. Some of these, however, may actually represent closely related but separate species, as recently shown for *M. pantanalense* from the Pantanal, upper River Paraguay system (dos Santos et al. 2013). In those inland populations, or cryptic species, reproduction is independent of salt water (Magalhães 1985; Zanders and Rodríguez 1992; Odinetz-Collart and Rabelo 1996; Anger and Hayd 2010). In the present study, we focused on a population originating from the Amazon estuary, near the type locality of *M. amazonicum* (Heller). All life-history stages of this population tolerated brackish and seawater (SW) conditions, being hyper-osmoregulators at salinities up to the iso-osmotic point (17 PSU), and hypo-regulators at higher salinities. Hyper-osmoregulation in FW, however, is absent or weak in the larvae (except for the first postembryonic stage, zoea I) and in early juveniles (Charmantier and Anger 2011). These ontogenetic patterns of osmoregulation and FW tolerance are congruent with a diadromous life cycle with hatching in rivers, a rapid passive zoeal downstream transport to brackish estuarine waters, where the subsequent larval development takes place, and later an active upstream migration of juveniles and adults.

At low salinities, a hyper-regulating organism is exposed to osmotic water influx and diffusive ion loss. At high salinities, a hypo-osmoregulating animal undergoes the reverse passive fluxes. The main sites involved in compensating these passive fluxes are the branchial chamber including the gills and the branchiostegites that are constantly exposed to the external environment (Charmantier et al. 2009). In fresh water, several working models for Na^+ and Cl^- uptake have been established and seem to differ between crustacean groups (reviewed by Charmantier et al. 2009; Henry et al. 2012; McNamara and Faria 2012). In *M. amazonicum*, working models for Na^+ absorption across the gill lamellae have been suggested; they involve pillar and septal cells that are structurally and functionally linked (McNamara and Torres 1999; Belli et al. 2009; Faleiros et al. 2010). Na^+ would enter pillar cells through apical ion exchangers and/or channels located in the extensive microvilli and it would pass through basal junctions into the septal cytoplasm from where it is actively exchanged for K^+ to the hemolymph via the Na^+/K^+-ATPase. Cl^- uptake is believed to depend on a functioning carbonic anhydrase and to proceed via apical $Cl^-/HCO3^-$ antiporter located in the pillar cells and basolateral Cl^- channels (McNamara and Faria 2012). These suggestions originate from previous models in other crustacean and fish species (Kirschner 2004; Freire et al. 2008; Evans 2008; Charmantier et al. 2009), but the exact mechanisms of chloride and sodium absorption are still unknown in palaemonid shrimps.

The V-type H^+-ATPase (V-H^+-ATPase) appears as a key enzyme for osmoregulation in many organisms (Forgac 1998; Beyenbach 2001; Kirschner 2004; Covi and Hand 2005). It was first isolated and characterized from intracellular vacuoles (Cidon and Nelson 1982; Moriyama and Nelson 1987), and it has later been located in the plasma membranes where in a variety of animals the enzyme energetizes secondary ion transport across whole epithelia by delivering protons from the cytoplasmic to the extracellular medium (Wieczorek et al. 1991; Beyenbach 2001). In hyper-osmoregulating organisms such as fresh water crustaceans, amphibians, and fish, an apical V-H^+-ATPase would be involved in driving ion uptake (Nelson and Harvey 1999; Wieczorek et al. 1999; Kirschner 2004; Beyenbach and Wieczorek 2006). In the posterior gills of the Chinese mitten crab, *Eriocheir sinensis*, an apical V-H^+-ATPase seems to be involved in electrogenic Cl^- absorption, as shown by significant decrease in net Cl^- influx across isolated and perfused gills after external application of bafilomycin, a

V-H^+-ATPase inhibitor (Onken and Putzenlechner 1995; Riestenpatt et al. 1995). Moreover, an apical V-H^+-ATPase might, as in frog skin (Ehrenfeld et al. 1990; Harvey 1992) or in several fish species (Wilson et al. 2000), support electrogenic apical Na^+ uptake (Kirschner 2004). The involvement of the V-H^+-ATPase in fresh water osmoregulation has been strengthened by studies on gene expression and protein activities (Faleiros et al. 2010; Lee et al. 2011; Towle et al. 2011). In *M. amazonicum*, the V-H^+-ATPase B-subunit mRNA expression decreased significantly after acclimation from fresh water to 21 PSU (Faleiros et al. 2010). The V-H^+-ATPase protein activity also decreases and becomes negligible after a 10 days acclimation period to 21 PSU (Faleiros et al. 2010). Similar results have been reported from a fresh water crab, *Dilocarcinus pagei* (Weihrauch 2004; Firmino et al. 2011), from an intertidal species of crab, *Uca formosensis* (Tsai and Lin 2007), and a copepod, *Eurytemora affinis* (Lee et al. 2011).

The subcellular location of the V-H^+-ATPase remains poorly explored in crustacean gills. Putzenlechner et al. (1992) were the first to localize V-H^+-ATPase in the pillar cells of *Eriocheir sinensis* gills (reviewed by Freire et al. 2008). Knowing the exact cell distribution in osmoregulatory epithelia would be a powerful support to better understand its involvement in ion transport. In the present study, using immunofluorescence and immunogold, we localized the V-H^+-ATPase in the gills and in the branchiostegites of the paleamonid shrimp *M. amazonicum* and investigated the effects of salinity variation on the main enzymes driving NaCl uptake (V-H^+-ATPase, Na^+/K^+-ATPase). The ultrastructure of gill lamellae and branchiostegites has been specified as well as effects of salinity on these epithelia.

Materials and methods

Origin and maintenance of animals

Adult *Macrobrachium amazonicum* originating from the Amazon estuary (Pará State, northeastern Brazil) were obtained from the State University of Mato Grosso do Sul in Aquidauana (Mato Grosso do Sul, MS, Brazil; for details, see Anger et al. 2009). Shrimps were transported in cooling boxes to the Helgoland Marine Biological Laboratory (Germany), where they were kept in fresh water (FW; total ion concentration 0.2 PSU; temperature 24°C; for more details, see Anger et al. 2009; Charmantier and Anger 2011). Adult shrimp were fed with frozen pieces of marine isopods (*Idotea* spp.) and commercial aquarium food (Novo Tab, JBL). Ovigerous females were maintained in aerated flow-through aquaria with 30 L of FW. Newly hatched larvae were collected in sieves (0.3 mm mesh size) receiving the overflowing water and subsequently reared in aerated 1 L beakers kept at 29°C and a 12:12 h light:dark cycle.

Salinity acclimation

Three-weeks-old (2.7 mm cephalothoracic length) and 5-months-old juveniles (4-5 cm total length) (referred to as early and late juveniles respectively) reared at 10 PSU salinity were stepwise transferred to FW (salinities 5, 2, 0.2 PSU) or to diluted seawater (DSW) (salinities 20, 25 PSU). Early and late juveniles were maintained for 2 weeks in FW or DSW.

Transmission electron microscopy (TEM)

Dissected pieces of gills and branchiostegites from FW and DSW acclimated late juveniles were fixed for 24 h at 4°C in glutaraldehyde (2.5%) in 0.1 mol/L sodium cacodylate buffer, pH 7.4, adjusted to the hemolymph osmotic pressure to prevent osmotic shocks. Samples were then rinsed (3x5 min) in sodium cacodylate buffer and postfixed for 1.5 h in osmium tetroxide at 1% in the same buffer on ice. Subsequent washings in distilled water and dehydration in graded ethanol series were followed by embedding in Epon resin. Transverse semithin (150 nm) and ultrathin (80 nm) sections were cut on the LKB BROMMA 8800 ultramicrotome. Semithin sections were stained with toluidine blue. Ultrathin sections were contrasted with aqueous uranyl acetate and lead citrate, and were observed at an accelerating voltage of 100 kV using a JEOL 1200 EX2 transmission electron microscope.

Quantitative measurements were derived from 3 animals. Six pictures from different gill lamellae have been taken from each animal using the same conditions. Values are expressed as (mean ± SD).

Western blots

The branchial chamber was dissected from early juvenile shrimps held either in FW or DSW; the epithelia were scraped on ice and homogenized in 500 µL of ice-cold SEI-PI buffer (0.1 mol/L imidazole; 0.02 mol/L EDTA; pH 7.4) containing 75 µL of protease inhibitors (PI) (Complete™, Mini, EDTAfree, Boehringer Mannheim GmbH, Penzberg, Germany) with a 1 mL Wheaton glass potter. After 1 h incubation on ice, homogenates were centrifuged at 2000 g for 6 min at 4 °C. Pellets were resuspended in 125 µL of 2.4 mmol/L sodium deoxycholate in SEI-PI buffer and centrifuged a second time (2000 g, 6 min, 4°C). The resulting supernatants were stored at −20°C. The protein content of the supernatants was determined using the Bradford method with a BSA (bovine serum albumin) standard. Twenty µg of protein samples were then separated under denaturing conditions on a 3% stacking and a 10% running polyacrylamide gel. The protein size marker was a Precision Plus Protein Standard (Precision Plus Protein™ Dual Color Standards, Bio-Rad, Marne-la-Coquette, France). Following the migration, proteins were transferred on a PVDF membrane (WESTRAN® Clear Signal, Schleicher and Schuell BioScience, Fontenay-sous-Bois, France) for 2 h 45 using a semi-dry transfer apparatus (Bio-Rad, Hercules, California, USA). Blots were blocked in Odyssey blocking buffer for 1 h at 37°C. The PVDF membrane was then exposed to the primary antibody (Guinea pig polyclonal antibody raised against the V1 domain of V-H^+-ATPase from *manduca sexta*) (Huss, 2001) at 1/1000 in Odyssey blocking buffer overnight at 4 °C. After two washes in PBS-T (0.1% Tween 20 in phosphate-buffered saline, pH 7.3) and one wash for 10 min in PBS at room temperature, the membrane was incubated for 1 h at room temperature with the secondary antibody at a 1/8000 dilution (IRDye® 800 CW conjugated donkey (polyclonal) anti-Guinea pig IgG; LI-COR, Biosciences, USA). Following three washes, the blots were visualized by immunofluorescence and the pictures were obtained using the Odyssey® imaging system.

Immunolocalization of V-H^+-ATPase and Na^+/K^+-ATPase

Early juvenile shrimps acclimated to FW or to DSW were fixed for 24 h by immersion in Bouin´s fixative. After rinsing in 70° ethanol, samples were fully dehydrated in a graded ethanol series and embedded in Paraplast (Sigma). Transverse sections (4 µm) were cut on a Leitz Wetzlar microtome, collected on poly-L-lysine coated slides and dried overnight at 37°C. Slides were then dewaxed (LMR), and rehydrated through a descending series of ethanol baths (100°, 95°, 90°, 70° and 50°) then were washed in PBS. Slides were incubated in sodium citrate buffer and microwaved (at 80% power 2 x 1 min) to reveal the antigenic sites. After cooling at room temperature, the slides were immersed for 10 min in a mixture of 0.01% Tween 20, 150 mM NaCl in 10 mM PBS, pH 7.3. Tissue saturation was performed by incubation in a solution of 5% skimmed milk SM-PBS for 20 min. Following three washes in PBS, the slides were incubated for 2 h at room temperature in a moist chamber with a mixture of the rabbit polyclonal Na^+/K^+-ATPase primary antibody at 8 µg/ml (SantaCruz Biotechnology, Cliniscience) and the Guinea pig polyclonal V-H^+-ATPase antibody at 1/100 dilution in 0.5% SM-PBS (Huss, 2001). Following washes, the slides were incubated with a mixture of secondary antibodies Rhodamine® donkey anti-rabbit IgG and AlexaFluor® 488 goat anti-Guinea pig IgG, (Invitrogen™) at 4 µg/ml and 10 µg/ml in 0.5% SM-PBS respectively for 1 h at room temperature. Control slides were exposed to the same conditions without primary antibody. After three washes, the slides were mounted in an anti-bleaching mounting medium (Gel/Mount, Permanent Aqueous Mounting, Biomeda, Plovdiv, Bulgaria) and observed with a Zeiss Axioimager® microscope equipped with a special filter for fluorescence (380 nm to 770 nm) and AxioVision 4© software.

Immunogold Electron Microscopy

Gills and branchiostegites from late juvenile shrimps acclimated to FW and DSW were fixed for 2 h with 2% paraformaldehyde and 0.5% glutaraldehyde in 0.1 M Na-cacodylate buffer, pH 7.5, adjusted to hemolymph osmolality of animals acclimated to FW or to DSW. After dehydration and embedding

in LR White, transverse ultrathin sections were cut on a Reichert TM60 ultramicrotome and collected on Formvar-coated nickel grids. Selected grids were hydrated in distilled water (5 min). The grids were successively preincubated on droplets of filtered PBS-BSA 2 % for 10 min and of normal goat serum at 1/30 for 30 min. The grids were then transferred to droplets of the primary antibody V-H^+-ATPase Guinea pig or Na^+/K^+-ATPase rabbit antibodies diluted to 1/150 or at 8µg/ml in 0.2% PBS-BSA, respectively, and incubated in a wet chamber one night at 4°C. The grids were washed in PBS-BSA (six times for 5 min) and incubated for 1 h in droplets of 20 nm gold-conjugated goat anti-Guinea pig IgG (abcam®) or 10 nm gold-conjugated goat anti-rabbit IgG (abcam®). After washing in PBS-BSA (three times for 5 min) and PBS (three times for 5 min), sections were stained with uranyl acetate (30 min) and examined with a JEOL 1200 EX2 transmission electron microscope. For controls, the procedure was the same but the grids were incubated without the primary antibody.

Results

Gill ultrastructure

No ultrastructural differentiation was noted when comparing the lamellae from different gills within an individual. Ultrastructural micrographs of *M. amazonicum* gills illustrate two main cell types: septal and pillar cells (Fig. 1b, c, d). A network of hemolymph lacunae is located between the two cell types, as shown in Fig. 1c, d, where two rows of symmetrical lacunae are visible on both sides of the septal cells. The septal cells contain a voluminous oval or round central nucleus (Fig. 1c, d) and their cytoplasmic membrane is highly amplified by deep and numerous infoldings associated with abundant mitochondria (Fig. 1d). The pillar cells are distributed on either side of the septal cells (Fig. 1c, d). The pillar cells present apical flanges that are lateral expansions extending under a thin cuticle, and which are in contact with adjacent flanges via junctional complexes (Fig. 1b, arrow). These flanges did not present any infoldings; mitochondria are present in the apical side of the flanges (Fig. 1c, d) but their number decreases toward their extremities (not shown). The hemolymph lacunae are detected at the basal sides of the flanges (Fig. 1b, c, d). The pillar cell bodies are rich in cellular organelles compared to the flanges and are in close contact with the septal cells. In some regions of the lamellae, two adjacent pillar cells connect to form a pillar (not shown).
In fresh water (FW), the apical surface of the pillar cells is highly amplified by an extensive system of microvilli associated with mitochondria and small vesicles (Fig. 1a, a′). These microvilli are observed above the perikaryon, becoming attenuated in the flanges (Fig. 1b). Acclimation to DSW (25 PSU) for 2 weeks induces various ultrastructural modifications in the gills such as a substantial decrease in the average thickness of the pillar cell flanges (1.34 µm ± 0.38, N=18) (Fig. 1c, d) compared to the fresh water condition (5.2 µm ± 1.03, N=18) (Fig. 1a, b) and an apparent decrease in the size and number of microvilli; only a few evaginations of the apical membrane are observed in DSW (Fig. 1d′). We did not observe any modification in the thickness of the intralamellar septal cells and of their structural organization between salinity conditions.

Branchiostegite ultrastructure

The branchiostegite comprises two epithelia separated by a wide hemolymph lacuna (Fig. 2a). The external epithelium is in close contact with the thick external cuticle; its thickness varies according to the molt stage (not shown). The internal epithelium, covered by a thin cuticle, presents ultrastructural features typical of an ion-transporting epithelium (Fig. 2a, b, c). Both epithelia are linked by pillar cells (Fig. 2a). In FW, the apical membrane of the cells lining the internal epithelium presents patches of microvilli associated with apical mitochondria (Fig. 2c, d) whereas the basal membrane forms many deep infoldings associated with abundant round or elongated mitochondria (Fig. 2c). Large and oval nuclei are located in the median zone. Irregularly shaped mitochondria can be observed around the nuclei (Fig. 2d). Acclimation to DSW induces ultrastructural modifications of the internal epithelium of the branchiostegite. The apical microvilli are absent (Fig. 2b, e) compared to those in FW. The basal infoldings are still present (Fig. 2b) but they seem less dense than in FW.

Western blotting

A polyclonal antibody raised against the native V1 domain of the V-H^+-ATPase from *M. sexta* (Huss, 2001) resulted in three main immunoreactive bands at 70 kDa, 56 kDa and 29 kDa (Fig. 3) using *M. amazonicum* gill homogenates. These protein bands were identified as subunits A, B and E of the V-H^+-ATPase by comparison with immunoreactive proteins of similar size in lysates of *M. sexta* and *Artemia franciscana* (Huss, 2001; Covi and Hand, 2005). Immunoreactive bands were absent on the blots incubated without primary antibody (not shown).

Immunolocalisation of V-H^+-ATPase and Na^+/K^+-ATPase

Control sections without the primary antibodies showed no immunolabeling (not shown). In gill lamellae of *M. amazonicum*, immunofluorescence micrographs showed positive V-H^+-ATPase immunoreactivity localized throughout pillar cells (Fig. 4a, b) without visible differences between salinities (25 PSU salinity not shown). Na^+/K^+-ATPase immunoreactivity was restricted to the septal cells (Fig. 4a′, b′). Double staining of V-H^+-ATPase and Na^+/K^+-ATPase showed no overlapping immunostaining (merge in Fig 4a″, b″). In the branchiostegite, V-H^+-ATPase and Na^+/K^+-ATPase colocalized in the same cells of the internal epithelium (Fig. 4b, b′, b″).

Using immunogold, negative control without the primary antibodies did not show any immunolabelling (Fig. 5e). Gill pillar cells reveal immunogold labelling of the V-H^+-ATPase at the apical microvilli (Fig. 5a, b) and also in clustered subapical areas suggesting labeling of vesicle membranes (Fig. 5c). The labeling density appears to decrease towards lateral expansions of the pillar cells (Fig. 5d). The septal cells expressed reduced V-H^+-ATPase immunogold labelling in all regions of the cell (not shown). In the branchiostegite, gold particles indicating the presence of V-H^+-ATPase were also localized in apical microvilli (Fig. 6a) and in electron-dense areas throughout the inner epithelium (Fig. 6b). Na^+/K^+-ATPase gold particles were localized densely along the basal infoldings of the cytoplasmic membrane (Fig. 6c). Negative control showed neither V-H^+-ATPase (not shown) nor Na^+/K^+-ATPase immunolabeling (Fig. 6d).

Discussion

The gill ultrastructure of *M. amazonicum* corroborates the previous descriptions of this organ (Belli et al. 2009; Faleiros et al. 2010) and the currently accepted palaemonid gill model (McNamara and Torres 1999; McNamara and Faria 2012), where ion transport mechanisms seem to be located in functionally different cell types. The lamellar epithelium consists of a pillar cells with extensive apical flanges and central septal cells, surrounded by hemolymph lacunae. This organization is similar to that observed in *M. olfersi* and *M. rosenbergii* (Freire and McNamara 1995; McNamara and Lima 1997; França et al. 2013). The gill pillar cells appear to be involved in salt transports, given their intimate connection with both the external medium and the hemolymph. In FW-acclimated *M. amazonicum*, their apical surface is highly amplified by extensive microvilli associated with mitochondria in the sub-apical cytoplasm. These microvilli increase the apical membrane area available for the insertion of transport proteins such as the ATP dependent V-H^+-ATPase, the close-by underlying mitochondria providing ATP to the enzyme. In the present study, we localized the V-H^+-ATPase by immunofluorescence and immunogold using a polyclonal antibody raised against the native V1 domain of the V-H^+-ATPase from *Manduca sexta*. The 3 bands that correspond to the subunits A (70 kDa), B (56 kDa) and E (29 kDa) in *M. amazonicum* blots have been previously detected in *Artemia franciscana*, where the same antibody has been used (Covi and Hand 2005). In *M. sexta*, supplementary bands have been detected (Huss, 2001).

In *M. amazonicum* gills, the V-H^+-ATPase was localized in the pillar cells only, both in the apical and cytoplasmic cell part, without visible differences between salinities. A similar pattern of localization of V-H^+-ATPase has been observed in gill pillar cells of the crab *Eriocheir sinensis* (Putzenlechner, 1994) but has never been shown in a Palaemonid shrimp. The cytoplasmic staining probably corresponds to intracellular vesicles, where the V-H^+-ATPase may play a role in their acidification (Beyenbach 2001; Kirschner 2004; Beyenbach and Wieczorek 2006). V-H+-ATPase activity and the V-H^+-ATPase B-subunit mRNA expressions have been quantified in *M. amazonicum* gill homogenates (Santos et al. 2007; Faleiros et al. 2010). According to these authors, a striking

decrease in V-H^+-ATPase activity and expression has been observed 10 days after acclimation of the shrimps to a salinity of 21 PSU. These findings point to the involvement of the V-H^+-ATPase in active Na^+ and/or Cl^- uptake in *M. amazonicum*, as generally accepted for fresh water-tolerant crustaceans (Freire et al. 2008; Charmantier et al. 2009). Moreover, in *Eurytemora affinis*, a copepod known as a rapid fresh water invader, evolutionary shifts in V-H^+-ATPase function following fresh water invasions have been observed; fresh water populations exhibited a more significant increase in V-H^+-ATPase activity in fresh water versus 15 PSU compared to saline populations (Lee et al. 2011). In *Callinectes sapidus*, the ENaC sodium channel inhibitor amiloride has been shown to inhibit unidirectional Na^+ influxes whereas it had no effect on Cl^- influx (Kirschner 2004). Research on isolated perfused gills of *E. sinensis* also showed independent electrogenic Na^+ and Cl^- influx (Péqueux and Gilles 1988; Onken and Graszynski 1989). Onken and Putzenlechner (1995) proposed an electrogenic uptake of Cl^- via apical $Cl^-/HCO3^-$ exchangers and basolateral Cl^- channels driven by an apical V-H^+-ATPase located in the apical microvilli of the pillar cells. Zare and Greenaway (1998) proposed a model where V-H^+-ATPase actively energizes Na^+ uptake in the gills of crayfish, *Cherax destructor*. Such different ion transport models proposed for different crustacean groups could be related to their differential evolutionary histories which may allow them to acquire variable adaptive strategies according to their habitats. Unlike in brachyurans, few studies are available on the osmoeffector proteins involved in hyper-osmoregulation in palaemonid species. In perfused *M. rosenbergii* gills, Torres (2006), using different inhibitors, showed that the V-H^+-ATPase might be functionally linked to Na^+ uptake through an apical Na^+ channel and/or Na^+/H^+ exchanger, and that carbonic anhydrase (CA) may provide the V-H^+-ATPase with H^+ (McNamara and Faria 2012). Whether chloride uptake also depends on V-H^+-ATPase in palaemonid species remains unknown.

We have shown in *M. amazonicum* that a transfer from FW to a salinity of 25 PSU results in a decrease in the number and length of the apical microvilli. This can be interpreted as a plastic phenotypic response to an exposure to high salinities, with a reduction of the membrane surface for ion exchange. The thickness of the pillar cell flanges is also reduced compared to those exposed to fresh water, suggesting that the gill epithelium is less permeable to ion loss at reduced salinity. Similar ultrastructural modifications have been observed in the gill epithelium of *M. olfersi* (McNamara and Lima 1997). Using immunogold, gold particles indicating the presence of V-H^+-ATPase are less concentrated in the flanges. These regions also appear less dense in organelles than the pillar cell bodies, suggesting that the flanges are probably more involved in respiratory gas-exchanges rather than in osmoregulation.

The intralamellar septal cells of *M. amazonicum* present typical features of ion transporting epithelia like those seen in the shrimp *M. olfersii* (McNamara and Torres 1999) and in several other crustacean species (Towle and Kays 1986; Péqueux 1995; review in Charmantier et al. 2009). The cell membrane exhibits a conspicuously augmented membrane system with deep infoldings in contact with the hemolymph associated with numerous mitochondria. We localized the Na^+/K^+-ATPase by immunohistochemistry in the septal cells. In *M. olfersi*, it was suggested that the multiple, stacked infoldings may hold salt transport to the hemolymph given the localization of Na^+/K^+-ATPase activity in this region (McNamara and Torres 1999). Recent studies have also mentioned the presence of Na^+/K^+-ATPase by immunofluorescence in the intralamellar septum of *M. rosenbergii* (França et al. 2013). In the palaemonid shrimp model, Na^+ is believed to enter the apical membrane of the pillar cell microvilli, cross the coupling junctions into the septal cell cytoplasm and pass into the hemolymph via the Na^+/K^+-ATPase system located in the deep membrane infoldings (McNamara and Torres 1999). In our study the strong immunofluorescence observed in the septal cells seems to corroborate this model. No visible differences were observed in Na^+/K^+-ATPase immunofluorescence labeling between salinities; however we know that gill Na^+/K^+-ATPase activity decreases in *M. amazonicum* following an exposure to a salinity of 25 PSU (Faleiros et al. 2010). Na^+/K^+-ATPase is believed to be involved in hyper- and hypo-osmoregulation in crustacean species. Its presence and low activity at high salinities might be sufficient to enable ion secretion. The NaCl secretion model has been well described in fish gills (Evans et al. 2005) and seems to involve a basal $Na^+/K^+/2Cl^-$ cotransporter (NKCC1). In *Macrobrachium* species, the Na^+/K^+-ATPase in the septal cell might generate an inward-directed Na^+ gradient that drives Na^+, Cl^- and K^+ transport through a NKCC cotransporter. Cl^- may exit via apical Cl^- channels in the pillar cells, creating a negative electrical potential that drives paracellular Na^+ efflux (McNamara and Faria 2012). Concerning the V-H^+-ATPase, our results showed that it is present

at 25 ppt and FW and no apparent difference in the localization and immunofluorescence intensity was recorded. Faleiros et al 2010 showed that the V-H^+-ATPase has a lower activity in 21 PSU acclimated shrimps compared to freshwater acclimated shrimps. Combining these two results we can propose that this low activity of V-H^+-ATPase at high salinity is not related to an absence of the protein but the V-H^+-ATPase seems not to be activated. This suggests that the V-H^+-ATPase is an enzyme that is post-transcriptionally regulated. However, more studies are necessary to fully understand the mechanisms involved in V-H^+-ATPase activation.
In this study, we provide evidence on the differential spatial distribution of the two main pumps involved in osmoregulation (V-H^+-ATPase and Na^+/K^+-ATPase) in *M. amazonicum* gills. Our data suggest that the highly differentiated pillar and septal cells form a cellular complex that is functionally linked in order to efficiently hypo-and hyperosmoregulate.

While the gills are known as the major osmoregulatory site that has been well documented in several species, fewer studies have been conducted on the branchiostegites, which also are believed to contribute to ion homeostasis (Felder et al. 1986). In *M. amazonicum,* the branchiostegites have been suggested as important sites for hypo-osmoregulation in larval stages given the high Na^+/K^+-ATPase abundance in the inner epithelium of an estuarine population (Boudour-Boucheker et al. 2013). The inner epithelium presents typical differentiations of an ion transporting epithelium: the apical cytoplasmic membrane presents patches of microvilli beneath a thin cuticle, and the basal cytoplasmic membrane forms many deep infoldings separating cytoplasmic areas that contain abundant round or elongated mitochondria. A similar ion transporting branchiostegite epithelium has been described in the caridean shrimps *Palaemon adspersus* (Martinez et al. 2005) and *Crangon crangon* (Cieluch et al. 2005), the peneid shrimp *Penaeus japonicus* (Bouaricha et al. 1994), and the lobster *Homarus gammarus* (Haond et al. 1998; Charmantier et al. 2001). One special feature of the inner epithelium of the branchiostegites in *M. amazonicum* exposed to FW is the close association between the abundant apical microvilli and numerous apical mitochondria, as in the pillar cells of the gills. This association has been previously described in ion transporting epithelia of insects (Harvey et al. 1981). In *Aedes aegypti* midgut, portasome-studded membranes near mitochondria have been observed through transmission electron microscopy. This provides evidence of an apical ion transport energized by the V-H^+-ATPase (Zhuang et al. 1999).

In *M. amazonicum*, acclimation to FW induces marked ultrastructural changes in the inner epithelium of the branchiostegite and an increase in the epithelium thickness, probably resulting from an increase in cell volume. We also detected a development of membrane infoldings, an increase in the number of mitochondria, the appearance of numerous large vesicles, and the development of apical microvilli. These structural features have also been reported from the osmoregulatory epithelia of other crustaceans maintained at low salinity (Haond et al. 1998), seemingly linked to hyper-osmoregulation. Unlike in gills, Na^+/K^+-ATPase and V-H^+-ATPase were co-localized in the same epithelial cells of the branchiostegite, suggesting that the underlying mechanisms of ion transport in this tissue are different from those in the gills. As shown by immunogold, Na^+/K^+-ATPase is located in the deep basal membrane infoldings, where it probably contributes to an increased active Na^+ uptake in fresh water. An increase in the number of mitochondria in these animals indicates higher energy requirements for enhanced active ionic transport processes. Na^+/K^+-ATPase was also localized in the inner epithelium of the branchiostegite of other decapod crustaceans such as the shrimp *Crangon crangon* and the crab *Eriocheir sinensis* (Cieluch et al. 2005; Cieluch et al. 2007). In *H. gammarus* subjected to a 20 PSU salinity, adjustment of the hemolymph osmolality correlates with increased specific activity of Na^+/K^+-ATPase in the epipodites and the branchiostegites, where it was 1.5 times higher than in the gills (Flik and Haond 2000; Charmantier et al., 2001). These findings, together with our results obtained in *Macrobrachium*, suggest that the branchiostegites play an important osmoregulatory role in the ability of crustaceans to adapt to salinity changes. To our knowledge, this study shows for the first time that V-H^+-ATPase is located in the branchiostegites, notably in the apical microvilli of the inner epithelium in *M. amazonicum* acclimated to fresh water. At a salinity of 20 PSU, the microvilli disappear and the density of gold particles in this region decreases. This suggests that, in fresh water, the presence of a membrane-associated V-H^+-ATPase is essential for energizing ion transport.

In conclusion, the gills and the inner side of the branchiostegites of *M. amazonicum* are formed by a well-differentiated ion transporting epithelium, and both house the two main pumps involved in ion transport. Our results suggest that the morphologically different cell types within gill lamellae may also be functionally specialized. We propose as a working hypothesis that, in FW, pillar cells expressing the V-H^+-ATPase absorb ions (Cl^-, Na^+) that are transported either directly to the hemolymph space or through a junctional complex to the septal cells. Septal cells housing Na^+/K^+-ATPase may be responsible for active Na^+ delivery to the hemolymph, which first passes through the pillar cells. This hypothesis suggests a clear functional link between septal and pillar cells to efficiently osmoregulate. When the shrimps are transferred to fresh water, gill and branchiostegite epithelia undergo considerable ultrastructural changes, most probably resulting from their involvement in adaptative osmoregulatory processes. Juvenile *M. amazonicum* are strong hyper-regulators in fresh water, maintaining hemolymph osmolality around 400 mOsm/kg. This ability may originate from the contribution of both pumps studied here, energizing ion uptake. Our findings, in conjunction with previous morphological and biochemical studies, provide a basis for a better understanding of the relative importance of V-type H^+-ATPase and Na^+/K^+-ATPase in disparate osmoregulatory challenges faced by juvenile *M. amazonicum* in estuarine habitats.

Acknowledgement

We thank Dr. Markus Huss and Prof. Helmut Wieczorek from the University of Osnabrück for providing the V-H+-ATPase antibody and Prof. Jehan-Hervé Lignot for his advice for immunogold.

References

Anger K (2001) The biology of decapod crustacean larvae. Crustacean issues 14. Balkema, Lisse

Anger K (2013) Neotropical *Macrobrachium* (Caridea: Palaemonidae): on the biology, origin, and radiation of freshwater-invading shrimp. J Crust Biol 33:151-183

Anger K, Hayd L, Knott J, Nettelmann U (2009) Patterns of larval growth and chemical composition in the Amazon River prawn, *Macrobrachium amazonicum*. Aquaculture 287:341–348

Anger K, Hayd L (2010) Feeding and growth in early larval shrimp *Macrobrachium amazonicum* from the Pantanal, southwestern Brazil. Aquatic Biol 9(3): 251-261

Bauer RT (2004) Remarkable Shrimps: Adaptations and Natural History of the Carideans. Norman, University of Oklahoma Press

Belli NM, Faleiros RO, Firmino KCS, Masui DC, Leone FA, McNamara JC, Furriel RPM (2009) Na^+ K^+-ATPase activity and epithelial interfaces in gills of the freshwater shrimp *Macrobrachium amazonicum* (Decapoda, Palaemonidae). Comp Biochem Physiol A 152:431-439

Beyenbach K (2001) Energizing Epithelial Transport with the Vacuolar H^+-ATPase. News Physiol Sci 16:145-151

Beyenbach K, Wieczorek H (2006) The V-type H^+-ATPase: molecular structure and function, physiological roles and regulation. J Exp Biol 209:577-589

Bouaricha N, Charmantier-Daures M, Thuet P, Trilles JP, Charmantier G (1994) Ontogeny of Osmoregulatory Structures in the Shrimp *Penaeus japonicus* (Crustacea, Decapoda). Biol Bull 186:29-40

Boudour-Boucheker N, Boulo V, Lorin-Nebel C, Elgero C, Grousset E, Anger K, Charmantier-Daures M, Charmantier G (2013) Adaptation to freshwater in the palaemonid shrimp *Macrobrachium amazonicum*: comparative ontogeny of osmoregulatory organs. Cell Tissue Res 353:87-98

Charmantier G, Anger K (2011) Ontogeny of osmoregulatory patterns in the South American shrimp *Macrobrachium amazonicum*: Loss of hypo-regulation in a land-locked population indicates phylogenetic separation from estuarine ancestors. J Exp Marine Biol Ecol 396:89–98

Charmantier G, Charmantier-Daures M, Towle D (2009) Osmotic and ionic regulation in aquatic arthropods. In: Evans DH (ed) Osmotic and ionic regulation: Cells and animals. Taylor and Francis Group, London, pp 165–208

Charmantier G, Haond C, Lignot J, Charmantier-Daures M (2001) Ecophysiological adaptation to salinity throughout a life cycle: a review in homarid lobsters. J Exp Biol 204:967–977

Cidon S, Nelson N (1982) Properties of a novel ATPase enzyme in chromaffin granules. J Bioenerg Biomembr 14:499–512

Cieluch U, Anger K, Charmantier-Daures M, Charmantier G (2007) Salinity tolerance, osmoregulation, and immunolocalization of Na^+/K^+-ATPase in larval and early juvenile stages of the Chinese mitten crab, *Eriocheir sinensis* (Decapod, Grapsoidea). Mar Ecol Progr Ser 329:169–178

Cieluch U, Charmantier G, Grousset E, Charmantier-Daures M, Anger K (2005) Osmoregulation, Immunolocalization of Na^+/K^+-ATPase, and Ultrastructure of Branchial Epithelia in the Developing Brown Shrimp, *Crangon crangon* (Decapoda, Caridea). Physiol Biochem Zool 78:1017–1025

Odinetz-Collart O, Rabelo H (1996) Variation in egg size of the fresh-water prawn *Macrobrachium amazonicum* (Decapoda: Palaemonidae). J Crust Biol 16:684–688

Covi JA, Hand S (2005) V-ATPase expression during development of *Artemia franciscana* embryos: potential role for proton gradients in anoxia signaling. J Exp Biol 208:2783–2798

Dos Santos A, Hayd L, Anger K (2013) A new species of *Macrobrachium* Spence Bate, 1868 (Decapoda, Palaemonidae), *M. pantanalense*, from the Pantanal, Brazil. Zootaxa 3700(3): 534–546

Ehrenfeld J, Lacoste I, Garcia-Romeu F, Harvey BJ (1990) Interdependence of Na^+ and H^+ transport in frog skin. In: Truchot JP and Lahlou B (ed) Animal nutrition and transport processes. Karger, Basel, Comp Physiol 6, pp 152-170

Evans DH (2008) Teleost fish osmoregulation: what have we learned since August Krogh, Homer Smith, and Ancel Keys. Am J Physiol Regul Integr Comp Physiol 295:704-713

Evans DH, Piermarini PM, Choe KP (2005) The Multifunctional Fish Gill: Dominant Site of Gas Exchange, Osmoregulation, Acid-Base Regulation, and Excretion of Nitrogenous Waste. Physiol Rev 85:97–177

Faleiros RO, Goldman MHS, Furriel RPM, McNamara JC (2010) Differential adjustment in gill Na^+/K^+- and V-ATPase activities and transporter mRNA expression during osmoregulatory acclimation in the cinnamon shrimp *Macrobrachium amazonicum* (Decapoda, Palaemonidae). J Exp Biol 213:3894–3905

Felder JM, Felder DL, Hand SC (1986) Ontogeny of osmoregulation in the estuarine ghost shrimp *Callianassa jamaicense* var. *luoisianensis* Schmitt (Decapoda, Thalassinidae). J Exp Mar Biol Ecol 99:91-105

Firmino KCS, Faleiros R, Masui DC, McNamara JC, Furriel RPM (2011) Short- and long-term, salinity-induced modulation of V-ATPase activity in the posterior gills of the true freshwater crab, *Dilocarcinus pagei* (Brachyura, Trichodactylidae). Comp Biochem Physiol B 160:24–31

Flik G, Haond C (2000) Na^+ and Ca^{2+} pumps in the gills, epipodites and branchiostegites of the european lobster *Homarus gammarus*: effects of dilute sea water. J Exp Biol 203:213–220

Forgac M (1998) Structure, function and regulation of the vacuolar (H^+)-ATPases. FEBS letters 440:258–263

França JL, Pinto MR, Lucena MN, Garçon DP, Valenti WC, McNamara JC, Leone FA (2013) Subcellular Localization and Kinetic Characterization of a Gill (Na^+, K^+)-ATPase from the Giant Freshwater Prawn *Macrobrachium rosenbergii*. J Membrane Biol, in press

Freire CA, McNamara JC (1995) Fine structure of the gills of the fresh-water shrimp *Macrobrachium olfersii* (Decapoda): effect of acclimation to high salinity medium and evidence for involvement of the lamellar septum in ion uptacke. J Crust Biol 15:103–116

Freire CA, Onken H, McNamara JC (2008) A structure–function analysis of ion transport in crustacean gills and excretory organs. Comp Biochem Physiol A 151:272–304

Haond C, Flik G, Charmantier G (1998) Confocal laser scanning and electron microscopical studies on osmoregulatory epithelia in the branchial cavity of the lobster *Homarus gammarus*. J Exp Biol 201:1817–1833

Harvey BJ (1992) Energization of sodium absorption by the H^+-ATPase pump in mitochondria-rich cells of frog skin. J Exp Biol 172:289–309

Harvey WR, Cioffi M, Wolfersberger MG (1981) Portasomes as Coupling Factors in Active Ion Transport and Oxidative Phosphorylation. Amer Zool 21:775-791

Heller C (1862) Beiträge zur näheren Kenntnis der Macrouren. Sitzungsberichte der mathematisch-naturwissenschaftlichen Classe der Kaiserlichen Akademie der Wissenschaften in Wien 1862: 389-426, Plates 381-382

Henry RP, Lucu C, Onken H, Weihrauch D (2012) Multiple functions of the crustacean gill: osmotic/ionic regulation, acid-base balance, ammonia excretion, and bioaccumulation of toxic metals. Front Physiol 3:1-33

Huss M (2001) Struktur, Funktion und Regulation der Plasmamembran V-ATPase von *Manduca sexta*. Ph.D. thesis, Universitat Osnabrück

Kirschner LB (2004) The mechanism of sodium chloride uptake in hyperregulating aquatic animals. J Exp Biol 207:1439–1452

Lee CE, Kiergaard M, Gelembiuk GW, Eads BD, Posavi M (2011) Pumping ions: rapid parallel evolution of ionic regulation following habitat invasions. Evolution 65:2229–2244

Martinez A, Charmantier G, Compère P, Charmantier-Daures M (2005) Branchial chamber tissues in two caridean shrimps: the epibenthic *Palaemon adspersus* and the deep-sea hydrothermal *Rimicaris exoculata*. Tissue Cell 37:153–165

Magalhães C (1985) Desenvolvimento larval obtido em laboratório de palaemonídeos da Região Amazonica. I. *Macrobrachium amazonicum* (Heller, 1862) (Crustacea, Decapoda). Amazoniana-Limnologia Et Oecologia Regionalis Systemae Fluminis Amazonas 9(2): 247-274

McNamara J, Moreira G, Moreira P (1983) The effect of salinity on respiratory metabolism, survival and moulting in the first zoea of *Macrobrachium amazonicum* (Heller) (Crustacea, Palaemonidae). Hydrobiologia 101:239–242

McNamara JC, Faria SC (2012) Evolution of osmoregulatory patterns and gill ion transport mechanisms in the decapod Crustacea: a review. J Comp Physiol B 182:997–1014

McNamara JC, Lima AG (1997) The Route of Ion and Water Movements Across the Gill Epithelium of the Freshwater Shrimp *Macrobrachium olfersii* (Decapoda, Palaemonidae): Evidence From Ultrastructural Changes Induced by Acclimation to Saline Media. Biol Bull 192:321–331

McNamara JC, Torres AH (1999) Ultracytochemical location of Na^+/K^+-ATPase activity and effect of high salinity acclimation in gill and renal epithelia of the freshwater shrimp *Macrobrachium olfersii* (Crustacea, Decapoda). J Exp Zool 284:617–628

Moreira GS, McNamara JC, Moreira PS (1986) The Effect of Salinity on the Upper Thermal Limits of Survival and Metamorphosis during Larval Development in *Macrobrachium amazonicum* (Heller) (Decapoda, Palaemonidae). Crustaceana 50:231–238

Moriyama Y, Nelson N (1987) The purified ATPase from chromaffin granule membranes is an anion-dependent proton pump. J Biol Chem 262:9175–9180

Nelson N, Harvey WR (1999) Vacuolar and plasma membrane proton-adenosinetriphosphatases. Physiol Rev 79:361–385

Onken H, Graszynski K (1989) Active Cl^- absorption by the Chinese crab (*Eriocheir sinensis*) gill epithelium measured by transepithelial potential difference. J Comp Physiol B 159:21–28

Onken H, Putzenlechner M (1995) A V-ATPase drives active, electrogenic and Na^+-independent Cl^- absorption across the gills of *Eriocheir sinensis*. J Exp Biol 198:767–774

Péqueux A (1995) Osmotic Regulation in Crustaceans. J Crust Biol 15:1–60

Péqueux A, Gilles R (1988) The transepithelial potential difference of isolated perfused gills of the Chinese crab *Eriocheir sinensis* acclimated to fresh water. Comp Biochem Physiol A 89:163–172

Pileggi, LG, Magalhães C, Bond-Buckup G, Mantelatto FL (2013) New records and extension of the known distribution of some freshwater shrimps in Brazil. Revista Mexicana de Biodiversidad 84: 563-574

Putzenlechner M, Onken H, Klein U, Graszynski K (1992) Electrogenic Cl^- uptake across the gill epithelium of *Eriocheir sinensis*: energized by a V-type ATPase? Verh Dtsch Zool Ges 85-160

Putzenlechner M (1994) Charakterisierung und Lokalisation einer Protonen-ATPase des V-typs in den Kiemen dekapoder Krebse (Crustacea, Dekapoda). Ph.D. thesis, Freien Universität, Berlin

Riestenpatt S, Petrausch G, Siebers D (1995) Cl^- influx across posterior gills of the Chinese crab (*Eriocheir sinensis*): potential energization by a V-type H^+-ATPase. comp Biochem Physiol A 110:235–241

Santos LCF, Belli NM, Augusto A, Masui DC, Leone FA, McNamara JC, Furriel RPM (2007) Gill (Na^+,K^+)-ATPase in diadromous, freshwater palaemonid shrimps: Species-specific kinetic characteristics and α-subunit expression. Comp Biochem Physiol A 148:178–188

Torres AH (2006) Um estudo eletrofisiológico e ultraestrutural do transporte iônico transepitelial em camarões e caranguejos (Crustacea, Decapoda). Ph.D. thesis, University of São Paulo

Towle DW, Henry RP, Terwilliger NB (2011) Microarray-detected changes in gene expression in gills of green crabs (Carcinus maenas) upon dilution of environmental salinity. Comp Biochem Physiol D 6:115–125

Towle DW, Kays WT (1986) Basolateral localization of Na^+ K^+-ATPase in gill epithelium of two osmoregulating crabs, *Callinectes sapidus* and *Carcinus maenas*. J Exp Zool 239:311–318

Tsai JR, Lin HC (2007) V-type H^+-ATPase and Na^+,K^+-ATPase in the gills of 13 euryhaline crabs during salinity acclimation. J Exp Biol 210:620 –627

Weihrauch D (2004) Ion-motive ATPases and active, transbranchial NaCl uptake in the red freshwater crab, *Dilocarcinus pagei* (Decapoda, Trichodactylidae). J Exp Biol 207:4623–4631

Wieczorek H, Grüber G, Harvey WR, Huss M, Merzendorfer H (1999) The plasma membrane H^+-V-ATPase from tobacco hornworm midgut. J Bioenerg Biomembr 31:67–74

Wieczorek H, Putzenlechnere M, Zeiskeg W, Klein U (1991) A Vacuolar-type Proton Pump Energizes K^+/H^+ Antiport in an Animal Plasma Membrane. J biol Chem 266:15340–15347

Wilson JM, Laurent P, Tufts BL, Benos DJ, Donowitz M, Vogl AW, Randall DJ (2000) NaCl uptake by the branchial epithelium in freshwater teleost fish: an immunological approach to ion-transport protein localization. J Exp Biol 203:2279–2296

Zanders IP, Rodríguez J (1992) Effects of temperature and salinity stress on osmoionic regulation in adults and on oxygen consumption in larvae and adults of *Macrobrachium amazonicum* (decapoda, palaemonidae). Comp Biochem Physiol A 101:505–509

Zare S, Greenaway P (1998) The Effect of Moulting and Sodium Depletion on Sodium Transport and the Activities of Na^+ K^+-ATPase, and V-ATPase in the Freshwater Crayfish *Cherax destructor* (Crustacea: Parastacidae). Comp Biochem Physiol A 119:739–745

Zhuang Z, Linser PJ, Harvey WR (1999) Antibody to H^+ V-ATPase subunit E colocalizes with portasomes in alkaline larval midgut of a freshwater mosquito (*Aedes aegypti*). J Exp Biol 202 (18): 2449-2460

Legends of Figures

Fig. 1 *M. amazonicum*. Ultrastructure of transverse sections of gill lamellae from late juveniles held in fresh water (a, a′ b) and diluted seawater at 25 PSU (c, d, d′). c: cuticle; f: flanges of pillar cell; h: hemolymph lacuna; i: membrane infoldings; m: mitochondria; mv: microvilli; n: nucleus; p: pillar cells; s: septal cells; arrow (b): junctional complex between two flanges. Scale bars: 5µm except for (a′, d′) 2µm

Fig. 2 *M. amazonicum*. Transverse semi-thin section of the branchiostegite from late juveniles (LJ) held in fresh water (FW) (a). Ultrastructure of the internal epithelium of the branchiostegite from LJ held in FW (c, d) and diluted seawater at 25 PSU (b, e). c: cuticle; h: hemolymph lacuna; i: membrane infoldings; ie: internal epithelium; m: mitochondria; mv: microvilli; n: nucleus; ee: external epithelium; p: pillar cells. Scale bars: 2 µm except for (a) 20 µm

Fig. 3 *M. amazonicum* early juveniles. Western blot analysis of the branchial V-H^+-ATPase after fresh water exposure. Molecular masses in kDa are indicated on the left

Fig. 4 *M. amazonicum*. Transverse sections of gill lamellae and branchiostegite from early juveniles held in fresh water. Pictures are taken with differential interference contrast (DIC). Immunolocalization of V-H^+-ATPase (green) (a,b) and Na^+/K^+-ATPase (red) (a′,b′). Merge of V-H^+-ATPase, Na^+/K^+-ATPase (a″,b″). br: branchiostegite; gl: gill lamellae. Scale bars: 20 µm

Fig. 5 *M. amazonicum*. Immunogold localization of V-H^+-ATPase in transverse sections of gill lamellae from late juveniles held in fresh water. The labeling is observed in the pillar cells (a). The labeling is distributed in the apical microvilli (b) and in the subapical region clustering in electron dense areas suggestive of a vesicular location (c). The density of immunogold labeling decreases towards the lateral expansions (d). Negative control without gold particles (e). The asterisk in (a) indicates an artifact. f: flange; h: hemolymph lacuna; mv: microvilli; n: nucleus; p: pillar cell. Scale bars: 1 µm

Fig. 6 *M. amazonicum*. Immunogold localization of V-H^+-ATPase and Na^+/K^+-ATPase in transverse sections of the branchiostegite from late juveniles held in fresh water. The labeling indicating the presence of V-H^+-ATPase (a, b) and Na^+/K^+-ATPase (c) is observed in the cells of the inner epithelium of the branchiostegite. V-H^+-ATPase is localized in the apical microvilli (a) and in cytoplasmic vesicles (b). Na^+/K^+-ATPase is localized along the basal membrane infoldings (c). Negative control of Na^+/K^+-ATPase without any gold particle (d). bi: basal membrane infoldings; c: cuticle; m: mitochondria; mv: apical microvilli; v: vesicles, Scale bars: 1 µm except for (c) 0.5 µm

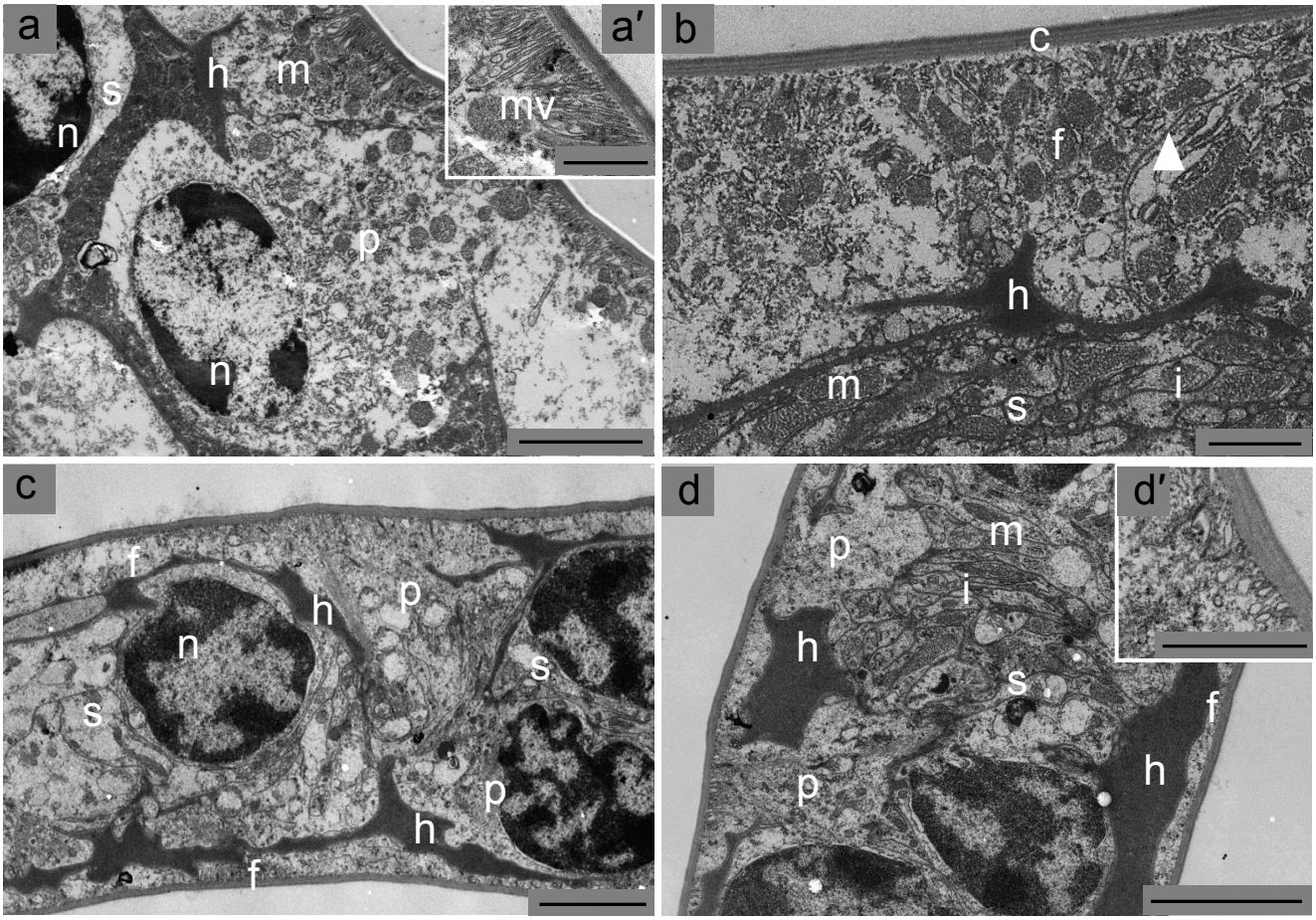
a
a′
b
c
d
d′
s
h
m
n
mv
p
c
f
i
h
m
s
i
f
h
p
n
s
s
p
h
f
p
m
i
h
s
f
h
p

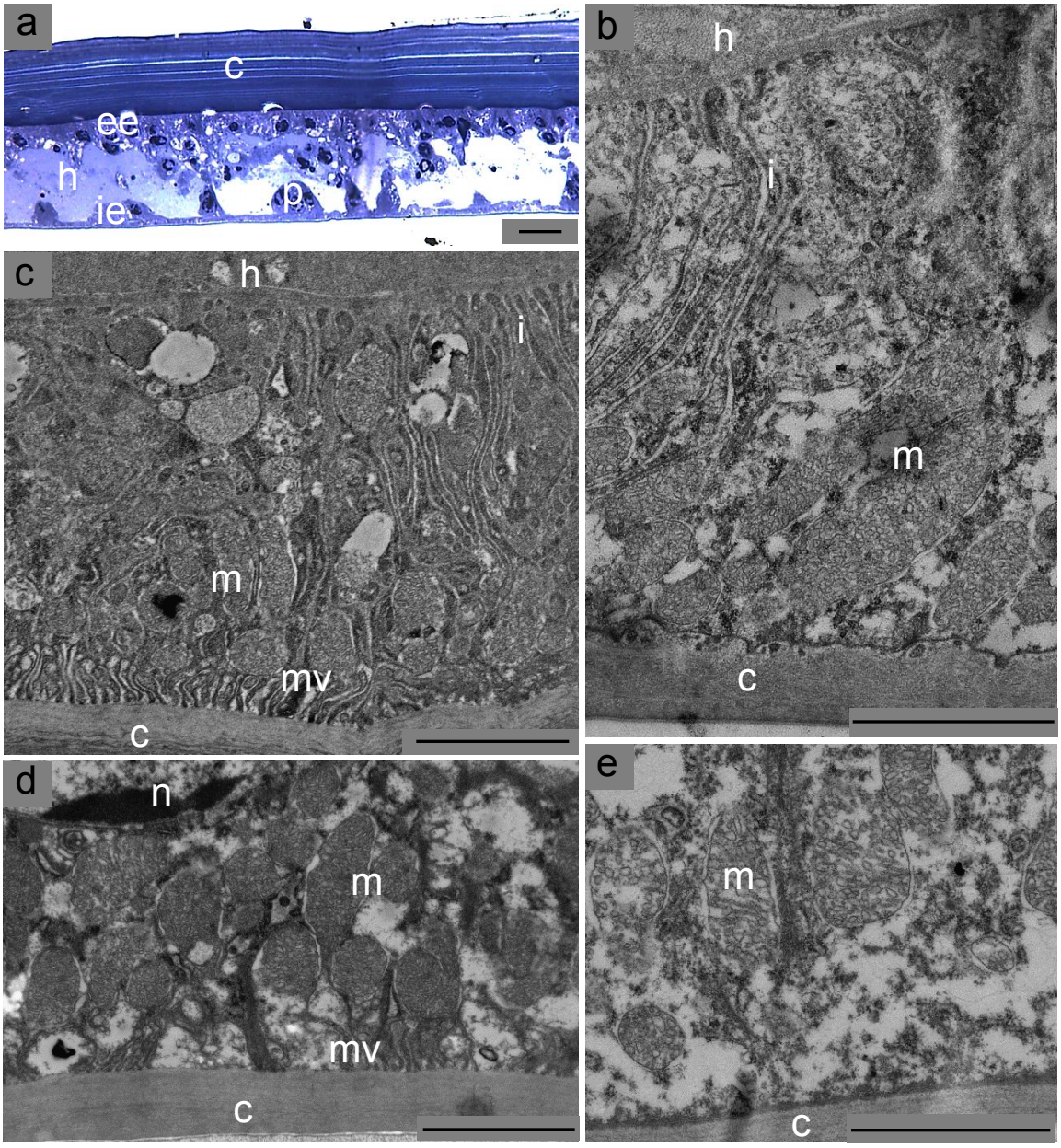
a
c
ee
h
ie
p
b
h
i
m
c
c
h
i
m
mv
c
d
n
m
mv
c
e
m
c

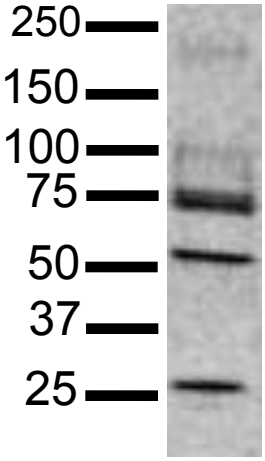
250
150
100
75
50
37
25

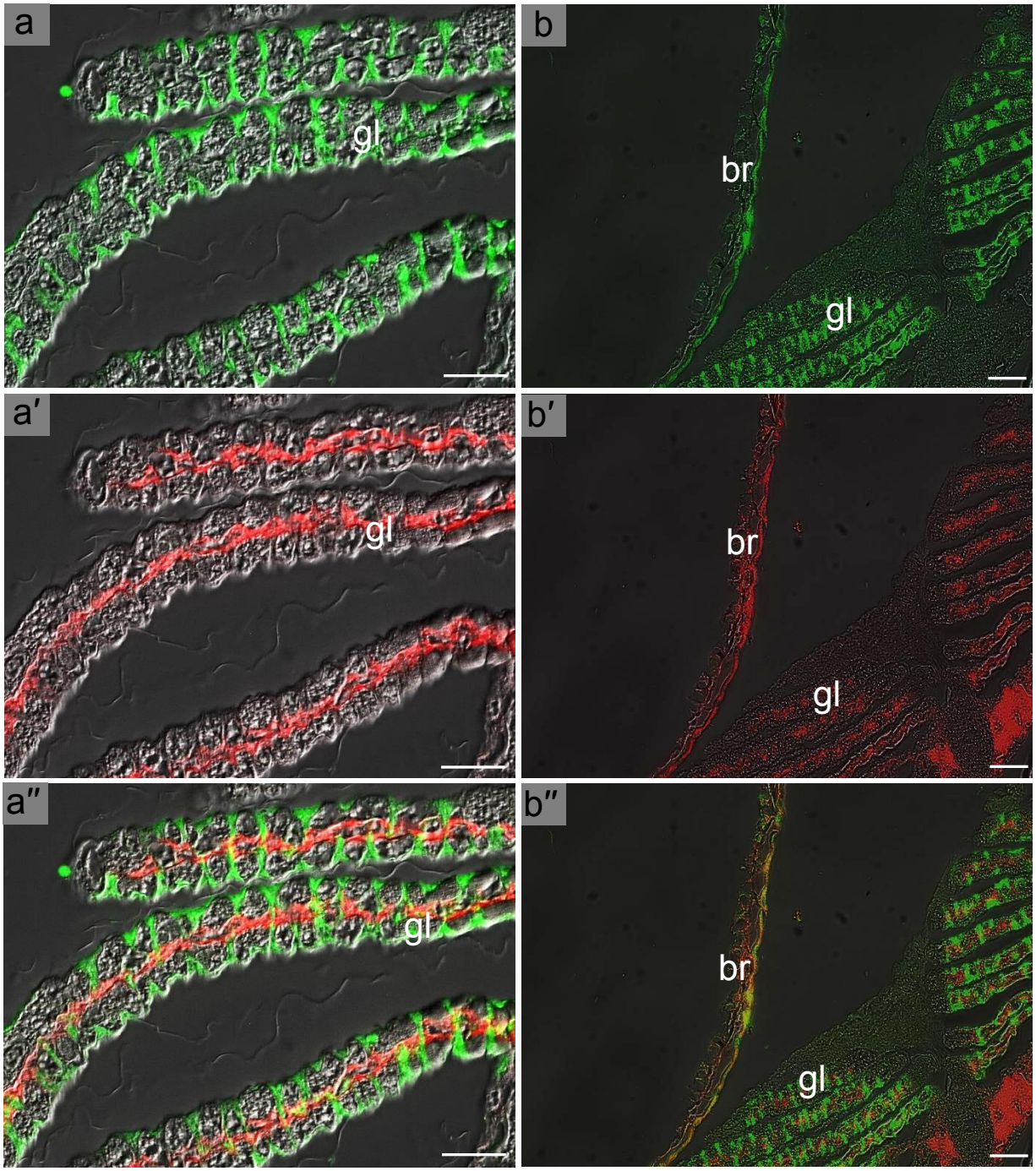
a
gl
b
br
gl
a′
gl
b′
br
gl
a″
gl
b″
br
gl

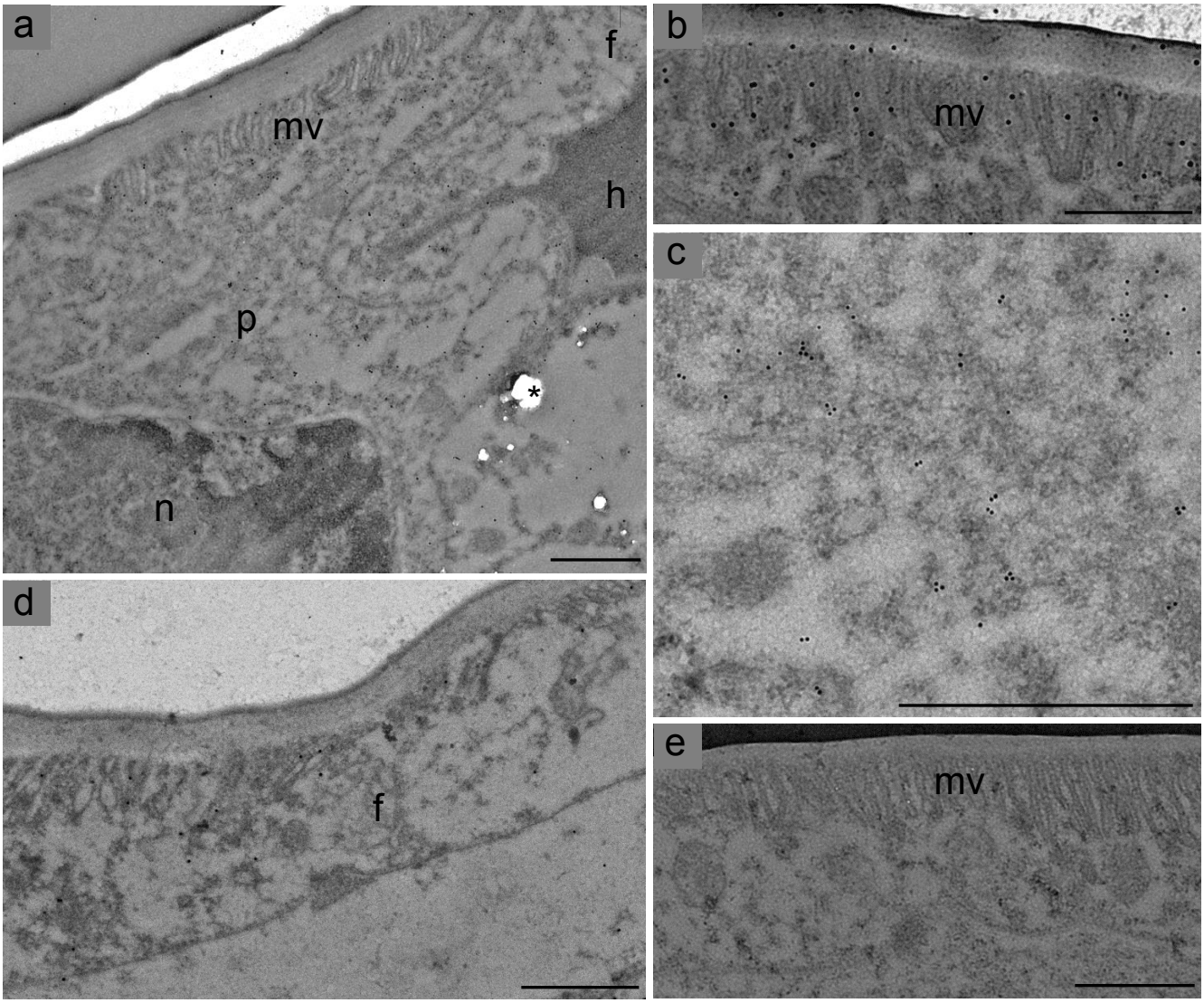
a
mv
f
h
p
*
n
b
mv
c
d
f
e
mv

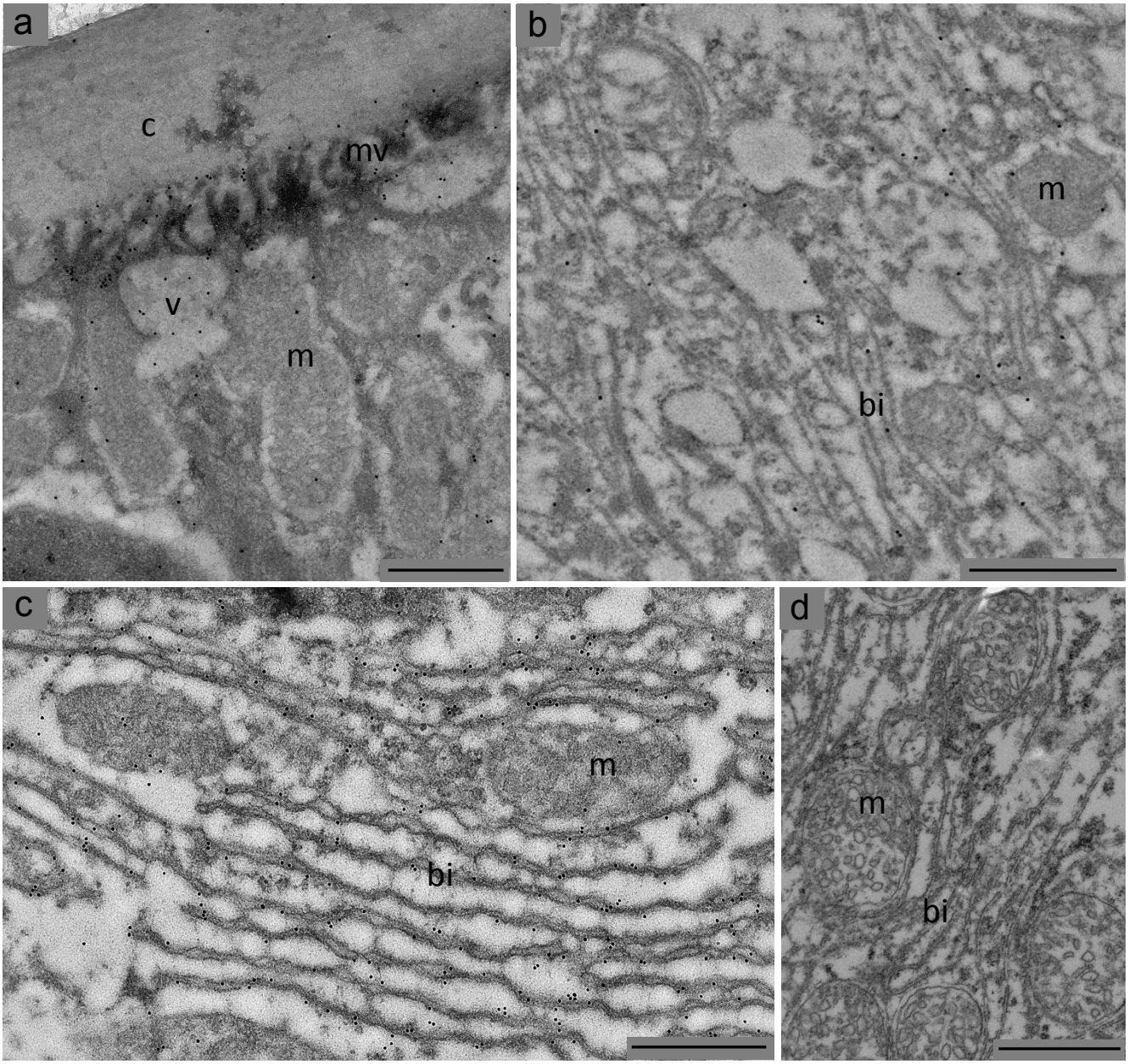
a
c
mv
v
m
b
m
bi
c
m
bi
d
m
bi